Springer

KSME

Journal of Mechanical Science and Technology 30 (5) (2016) 2265~2271
www.springerlink.com/content/1738-494x(Print)/1976-3824(Online)
DOI 10.1007/s12206-015-0843-1

Modular design and control of an upper limb exoskeleton †

Javier Garrido[1], Wen Yu[1,*] and Xiaoou Li[2]

[1]*Departamento de Control Automatico, CINVESTAV-IPN (National Polytechnic Institute), Mexico City, 07360, Mexio*
[2]*Departamento de Computacion, CINVESTAV-IPN (National Polytechnic Institute), Mexico City, 07360, Mexico*

(Manuscript Received September 10, 2014; Revised April 20, 2015; Accepted May 25, 2015)

Abstract

In this paper, we use modular design method to construct an upper limb exoskeleton. This new design method is more simple and easy for exoskeletons than the other techniques, and it is facility to be extended into more joints robots. We also propose a novel admittance control, which works in task space. The admittance control has PID form, and does not need the inverse kinematic and the dynamic model of the exoskeleton. The experimental results show that both the design and the controller work well for the upper limb exoskeleton.

Keywords: Admittance control; Modular design; Robot exoskeleton; Upper limb

1. Introduction

The wearable robot such as exoskeleton combines the human and the robot into one integrated system under the control of the human. It leads to a solution which benefits from the advantages of each sub-system. The heart of this human-machine integration has two fundamental scientific and technological issues: the exoskeleton mechanism itself and its biomechanical integration with the human body [1]. There are three fundamental applications: device for teleoperation [2], human-amplifier [3], and physical therapy modality as part of the rehabilitation [4]. The exoskeleton robots can be divided into upper limbs [3] and lower limbs [5].

A simplified model of human arm has 7 Degree-of-freedom (7-DoF). Many upper limb exoskeletons have 7-DoF [6]. These redundant robots [7] robot neglect translational and rotational motion of the scapula and clavicle of human arm. The 7-DoF arm model give a good combination of motion accuracy while reducing the model complexity to a manageable level. More complex upper limb exoskeletons, such as 9-DoF [8] and 11-DoF [9] robots, are not popular, because the additional joints do not provide more functions. The human arm kinematics and dynamics during activities of daily living are studied in part to determine the engineering specifications for the exoskeleton design. Although great progress has been made in a century-long effort to design and implement robotic exoskeletons, many design challenges continue to limit the performance of the system. If only the motions of the shoulder and the elbow are considered, the human arm has 4-DoF. This 4-DoF includes most of human arm motions. There are some 4-DoF exoskeleton robots [10].

In order to control an exoskeleton, the interface between the human and the mechanical system is needed. This interface, particularly in the field of hepatics, maps human force into a motion. The input of an admittance is force and the output is velocity or position. In other words, an admittance device would sense the input force and "admit" a certain amount of motion. Path tracking accuracy and contact forces are two contradiction objectives in stiffness control [11] and force control [12]. Improvement of the position tracking accuracy might give rise to larger contact forces. The force/position control [13] and impedance control [14] used inverse dynamic such that the task space motion is globally linearized and decoupled, and asymptotically stable. In Ref. [8], two three-axis force sensors is used for admittance control of the upper and lower arm segments. It uses the top half of the Jacobian to compute the forces and torques of the human arm.

However, all above impedance/admittance need robot models. The model for the exoskeleton include forward kinematic, inverse kinematic, and dynamic model. The kinematics are used to calculate the relation between the joint angles and the arm position, while the dynamic model is applied to design controllers. It is impossible to design a model-based impedance/admittance control when a complete dynamic model of the robot is unknown [15]. The contributions of the paper are in two parts: a) Modular design for robot exoskeleton, the advantage is the design process is more simple and easy than the other exoskeletons. see Fig. 1. b) Novel admittance control,

*Corresponding author. Tel.: +52 55 54473734, Fax.: +52 55 57473982
E-mail address: yuw@ctrl.cinvestav.mx
† Recommended by Associate Editor Kyoungchul Kong

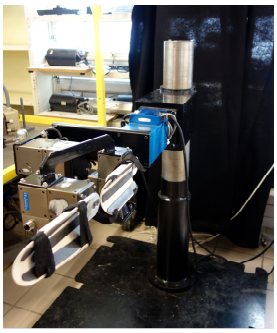

Fig. 1. A 4-DoF upper limb exoskeleton.

this controller works in task space, so it does not need the inverse kinematic of the exoskeleton. This controller is also transformed into PID form, so it does not needs the dynamic model of the exoskeleton.

2. Modular design of upper limb exoskeleton

2.1 Kinematics and dynamics of the human arm

The design of the upper limb exoskeleton is based on the kinematics and dynamics of the human arm during activities of daily living. Human upper limb is composed of segments linked by articulations with multiple degrees of freedom. It is a complex structure that is made up of both ridged bone and soft tissue. This soft tissue moves and slides relative to the bone during movements and interactions with the environment. Additionally, muscle contractions cause changes to their shape and the over all stiffness of the arm. Although much of the complexity of the soft tissue is difficult to model, the overall arm movement can be represented by a much simpler model composed of ridge links connected by joints.

Three ridged segments, consisting of the upper arm, lower arm and hand connected by frictionless joints make up the simplified model of the human arm. Placing a reference frame at the shoulder, the upper arm and torso are rigidly attached by a ball and socket joint. This joint is responsible for three shoulder motions: abduction-adduction, flexion-extension and internal-external rotations. The connection between the upper and lower arm segments can be regarded as a single rotational joint at the elbow, see Fig. 2. The shoulder is a spherical joint, which includes shoulder abd-add, shoulder flex-ext, and shoulder int-ext rotation. The elbow has two rotation: elbow flex-ext and pronation-supination. The wrist can be also defined two rotations: wrist flex-ext and wrist radial-ulnar deviation. In order to simplify the design process, the pronation-supination of the elbow is moved to the wrist. So the elbow only has flexion-extension rotation, and the lower arm and hand are connected by a spherical joint resulting three wrist motions.

2.2 Mechanics design of upper limb exoskeleton

The fundamental principal in designing the exoskeleton

Table 1. Physics parameters of the four links.

Link	Mass (g)	Dimension (mm)
1	2875	Long: 345, width: 228, high: 100
2	1578	Long: 190, width: 175, high: 100
3	1576	Long1: 345, widthl: 228, long2: 220, width2: 95
4	2115	Longl: 220, widthl: 95, 1ong2: 220, width2: 72

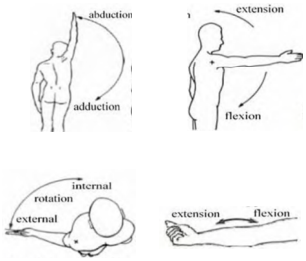

Fig. 2. Four basic motions of human arm.

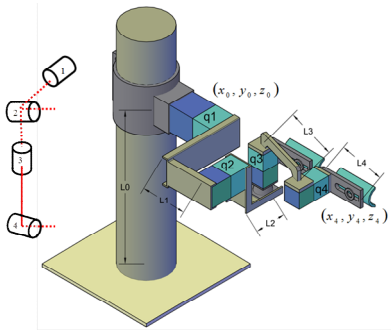

Fig. 3. Joint configuration and DoF selection.

joints is to align the rotational axis of the exoskeleton with the anatomical rotations axes. If more than one axis is at a particular anatomical joint, for example the spherical joint of shoulder or wrist, the three axes must be intersected, and the elbow axis is orthogonal to the third shoulder axis. The pronation-supination takes place between the elbow and the wrist as it does in the physiological mechanism. The simplification of this paper support 99% of the ranges of motion required to perform daily activities [1].

The joint configuration and DoF selection are shown in Fig. 3. This configuration satisfies two basic requirements: 1) All of their rotation axes are orthogonal (ball joint), 2) the three rotation axes are intersected in one point. In order to simulate the motions of abduction-adduction, flexion-extension and internal-external rotations, the special link pieces are designed , such that these three links satisfy the basic requirements of the human upper limb. The links L0 and L4 are adjustable. L0 is for different height of persons, L4 is different length of human arms. The users left hand is an enable button which released the brakes on the device and engaged the motor.

Table 1 gives the physics parameters of the four links. The thickness of all links are 4.76 mm.

The safety steps includes the mechanical, electrical and

Fig. 4. Standard rotary module: PowerCube.

software designs. In the mechanical part has a physical stops prevent segments in the joints. The electrical part is added an emergency shutoff button to terminate motor motion. The most easy method is to use software to monitor power transmission integrity to limit motor currents, i.e., motor torques. When the motor moves near to the limits, a brake command is send to this motor, via software is selected maxim and minimum range of degree for the movements for each one.

2.3 Modular design of actuation

The concept of the exoskeleton design in this paper is the exoskeleton is divided into: joint (actuation), link, and control system. Each sub-system has its own function and can be independently tested. This design allows us to increase or reduce DoF directly, for example from the 4-DoF exoskeleton of this paper to the 7-DoF exoskeleton [1]. The advantages of this design are saving time, reduction in cost, and flexibility in design. The rotational DoF is actuated by the PowerCube unit. The cubic geometry makes the system extremely adaptable for modular solutions. The benefit of this unite for our modular design is it can be mounted one four sides, see Fig. 4. This overcomes the frequent changes of customer demands, and make the manufacturing process more adaptive to the change. The PowerCube unit has a brushless EC motor. The transmission of this unite is a harmonic drive.

The harmonic drive has three types of motions by combinations of the three components: high speed rotation, low speed rotation, and high torque rotation. The PowerCube unit uses the high torque rotation, where the Flex spline is fixed and the Wave generator is transmitted through the Circular spline. So the servo positioning module combines high precision and high torque, and have a very compact design. The high torques are achieved by the integrated harmonic drive gears with considerable reserves of acceleration and deceleration, while the high-resolution encoder guarantees high precision. If the transmission ratio of the harmonic drive N, which the positions of two components. The ideal rotation of the third component is

$$\theta_{WG} = (N+1)\theta_{CS} - N\theta_{FS} \quad (1)$$

where θ_{WG}, θ_{CS} and θ_{FS} are the rotations of the wave generator, the circular spline, and the flex spline. If $\omega_{cs} = 0$,

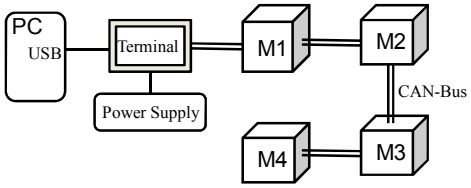

Fig. 5. Control system.

the wave generator rotates N times faster than the flex spline in the opposite direction. A fixed flex spline wave generator causes the rote (N+1) times faster than the circular spline in the same direction.

2.4 Control system

All of actuation modules are connected by CAN bus (Controller Area Network), which uses single-cable technology to integrate the existing modules, see Fig. 5. CAN allows microcontrollers and devices to communicate with each other without a host computer. The module can have a single CAN interface rather than analog and digital inputs to every device in the system. This decreases overall cost and weight of each joint. The new module can quickly be integrated into existing systems using the universal communication interfaces CAN.

CAN communicates with PC with DSPIC30F4012 card or USB port. It is a message oriented protocol. Each message has a unique identifier within the network, in which nodes choose to accept or reject the message. Protocol of CAN includes three layers: physical layer, data link layer and special coating for management (control node layer). CAN solve the simultaneous transmission problem by assigning priorities by the identifier of each message. The identifier with the lowest binary number is the highest priority. The medium access methods used in CAN are Carrier sense multiple access (CSMA), Collision detection (CD) and Arbitration on message priority (AMP). If a node in the network needs to transmit information, it must wait until the bus is free. When this condition is met, this node transmits four types of frames: Remote frame, error frame, extended frame and overload frame.

The hand HMI consists of a handle, the upper and lower arm HMI consists of a pressure distributive structural pad that securely strapped to the mid-distal portion of each respective arm segment. Compliance of relaxed musculature in proximal regions of the limb, as well as non-uniform transformations during muscular contraction, reduce interfacial stiffness and produce higher non-linear disturbances in force measurements, which would ultimately result in reduced bandwidth of performance. Cross section of distal parts of limb segments are less variable in magnitude and experience fewer underlying skeletal transformations, making them better for HMI attachments. Each interface is rigidly attached to a force/torque sensor that is in turn rigidly attached to the exoskeleton, see Fig. 6. These sensors allow every force and torque interactions between the exoskeleton and the user to be measured.

Fig. 6. The handle for the human machine interface.

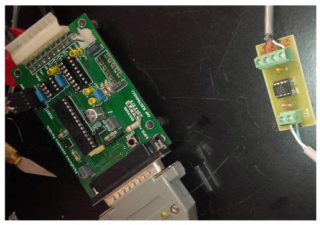

Fig. 7. Interface card of USB and CAN.

3. Admittance control of the upper limb exoskeleton

The object of admittance control is to generate reference trajectories for each joint, such that the upper limb exoskeleton moves as the human wants. The human uses the handle to generate three forces and three torques signals $f_e \in R^6$. When the exoskeleton's end-effector contacts the environment, a task space coordinate system defined with reference to the environment is convenient for the study of contact motion. With the force on the end-effector, the dynamic of the exoskeleton robot (dynamic) becomes

$$M(q)\ddot{q} + C(q,\dot{q})\dot{q} + G(q) + F(\dot{q}) = \tau - J^T f. \tag{2}$$

In this paper, we only consider arm motion. The 3 DoF in hand is not included in the exoskeleton. The dimension of q is four, and $J \in R^{4\times 4}$ is the Jacobian matrix, $f \in R^4$ represents the contract force and torque in the end-effector. The output of the force sensor $f_e = \left[f_x, f_y, f_z, \tau_x, \tau_y, \tau_z\right]$, we do not consider two torques $\left[\tau_y, \tau_z\right]$. $f_e = \left[f_x, f_y, f_z, \tau_x\right] \in R^4$.

Let $x_e \in R^6$ be the task space vector defined by $x_e = K_e(q)$, where x_e is position and orientation of the end effector in base coordinates. $K_e(\cdot) \in R^6 \to R^6$ is the forward kinematics of the robot, which is a nonlinear transformation describing the relation between the joint and task space. The Cartesian velocity vector $\dot{x}_e = \left[u^T, v^T\right]^T \in R^6$, $u \in R^3$ is the linear velocity, $v \in R^3$ is the angular velocity. In this paper, the exoskeleton only has 4-DoF. We use three position and one orientation for the end effector, i.e., $x \in R^4$, $x = K(q)$, $K(\cdot) \in R^4 \to R^4$. This model is only for controller analysis, we do not use it for controller design. We use the force sensor at the end effector to generate reference position and orientation x. We use the idea of impedance. The mechanical impedance describes a force/velocity relation of the end-effector,

$$\frac{f(s)}{\dot{x}(s)} = M_i s + B_i + \frac{D_i}{s} = Z(s) \tag{3}$$

where f represents the force exerted on the environment, $\dot{x}$ represents the velocity of the manipulator at the environmental contact point. Z represents the environmental impedance, M_i, B_i and D_i are the inertia, viscosity and stiffness of the end-effector, respectively. When robot dynamic is known, the traditional impedance control is

$$u = M(q)J^{-1}\left(a - \dot{J}\dot{q}\right) + C(q,\dot{q})\dot{q} + g(q) + J^T(q)f$$
$$a = \ddot{x}_d + \frac{B_i}{M_i}\left(\dot{x}_d - \dot{x}\right) + \frac{D_i}{M_i}\left(x_d - x\right) - \frac{f}{M_i}$$

the parameters M_i, B_i and D_i are designed such that the closed-loop system

$$M_i\left(\ddot{x}_d - \ddot{x}\right) + B_i\left(\dot{x}_d - \dot{x}\right) + D_i\left(x_d - x\right) = f.$$

The impedance control Eq. (3) can generate reference signal as

$$x_d(s) = \frac{1}{M_i s^2 + B_i s + D_i} f(s) \tag{4}$$

Eq. (4) is called as impedance filter [16]. The impedance characterization of the human arm [17] and biomechanical data [18] can help us to select the right inertia and damping parameters M_i, B_i, and D_i in Eq. (4). However the impedance filter can cause user discomfort with small differences in exoskeletons position and the users desired position, because the impedance filter cannot guarantee zero contract force.

The admittance relation is the inverse of Eq. (3),

$$\frac{\dot{x}(s)}{f(s)} = M_a s + B_a + \frac{D_a}{s} = R(s) \tag{5}$$

where f represents force and torque of the force sensor, M_a, B_a and D_a are design parameters for admittance control.

4. Experiment results

The computer control platform for our upper limb exoskeleton, CINVESRobot-1, is shown in Fig. 1. The computer is an Intel Pentium 4 @2.4GHz processor, and 2G RAM. The operation software are Windows XP with Matlab 7.2 + WinCon. The real-time control programs also operated in Real-time target. The communication interface is USB with CAN bus with DsPic, see Fig. 7.

The running frequency of the CPU processor in each module is 1.0 GHz processor. The communication rate of the CAN

Fig. 8. 6-axis force/torque sensor with a data acquisition system.

bus is set as 5 K bps. We use 500 Hz as the sampling frequency as the control loop. So the sampling/control speed is much lower than the modules and their communication rate. In this way, each module has enough time to finish its job assigned by the upper PC, and send back the positions to the PC. CAN bus does not have a separate clock signal for synchronization. When the bus is idle, the synchronization starts, and re-synchronization occurs on every recessive to dominant transition during the frame. So all nodes on the CAN bus operate at the same bit rate with respect to noise, phase shifts and oscillator drift. The users left hand is an enable button which released the brakes on the device and engaged the motor. We use three types modules for the four joints: PowerCube PR110, PR90, and PR70. The power supply for PR110 is 48 VDC, and for PR90 and PR70 are 24 VDC. The normal torques of them are 142 Nm, 72 Nm and 23 Nm. The weight of these modules are 5.6 Kg, 3.4 Kg and 1.7 Kg. The first joint of the 4-DoF exoskeleton is mounted on the ground. It needs to hold all other joints. The dimension of the exoskeleton is about 1 m. The maximum load for Joint-1 is about 15 kg, i.e., it can other two PR90 and five PR70 modules. The second joint of this exoskeleton uses PR90 module. The third and forth joints use PR70 module. The Joint-2 can be connected by the other five PR70 modules. Joint-3 can hold 7.8 Kg, if the dimensions of Joint-4, Joint-5, etc., are estimated as 0.3 m. So Joint-3 can be connected by another PR70 module. The human-machine interface is a 6-axis force/torque sensor, Mini40 F/T sensor (ATI Industrial Automation). This sensor system includes a data acquisition system. It send digital signals of three forces and three torques to computer via the RS232 serial port, see Fig. 8.

The real-time control program operated in PC is Matlab with Real-time target and C. For each module, it has its own control loop. It is PID control. For this exoskeleton, overshot is not permitted, while long rise time is possible. From Table 5, we use the following PID parameters

$$\begin{aligned} K_p &= [15,15,10,15] \\ K_i &= [2,1,2,2] \\ K_d &= [330,330,300,320]. \end{aligned} \tag{6}$$

The step response of the four joints (motors) are shown in Fig. 9. Here the red lines are references, the black lines are the

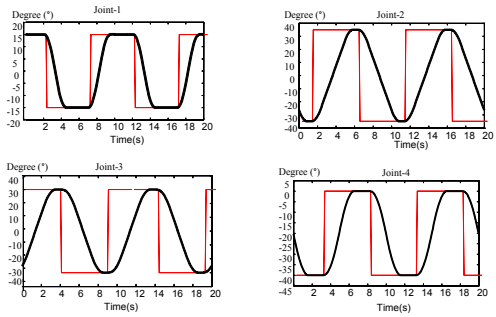

Fig. 9. Step responses of the four motors.

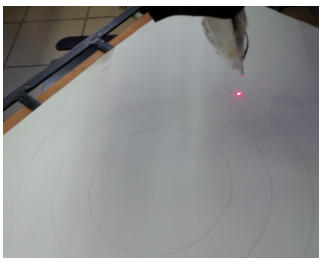

Fig. 10. The orientation of the end-effector.

rotation angles of the motors. We can see that the lower level position regulation of the joints works very well.

The second experiment is to draw several "8". In order to control the 4-DoF exoskeleton, we use three forces $[F_x, F_y, F_z]$ and one torque T_x as the input f_d. The admittance control is to generate desired trajectories of the four joints from f_d, and the move the end-effector of the exoskeleton robot from an initial position into desired position. The PID admittance control in task space is

$$\dot{x}_d = B_a f_d + D_a \int_0^t f_d(\upsilon) d\upsilon + M_a \dot{f}_d \tag{7}$$

where B_a, D_a and M_a are human impedance parameters, which depend on each one feeling. In this paper, we select

$$\begin{aligned} B_p &= diag[124,120,50,120,50,70,70] \\ D_a &= diag[2,1,2,2,0.2,0.1,0.1] \\ M_a &= diag[410,410,200,300,410,200,200]. \end{aligned}$$

Here the forces $[F_x, F_y, F_z]$ generate three-dimension trajectories $[x, y, z]$, while the torque T_x gives the orientation of the end-effector, see Fig. 10.

The three forces are regulated by the admittance control Eq. (7), and generate references for the joints, see Fig. 11. The lower level PID control can force the motors to follow these references. The trajectory of the end-effector in the tasks pace is shown in Fig. 12. Here the trajectory in 3D space is calculated from forward kinematic of the exoskeleton, because we do not have effective 3D motion tracking system to show it. We can see that the upper limb exoskeleton can be controlled

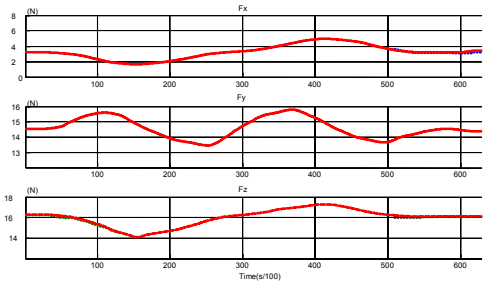

Fig. 11. Three force commands.

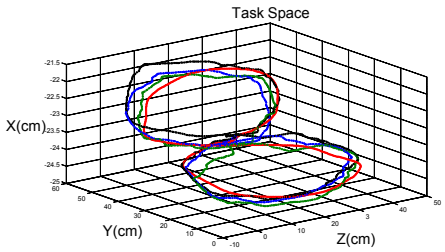

Fig. 12. The trajectory of the end-effector.

by a force sensor, and move freely. It can draw a "8" within 6 seconds. The accuracy of the movement depends on the human model, i.e., the human has to transfer a 3D "8" into corresponding forces. This should be the inverse model of PID admittance control. However, Eq. (7) is too simple to describe complex human behavior. At least, the novel PID admittance control proposed in this paper works well for simple motions.

5. Conclusions

In this paper, we use modular design to construct a 4-DoF upper limb exoskeleton. This new design method process for exoskeletons is more simple and easy than the other exoskeleton design techniques, and it is facility to be extended into more joints robots. We also propose a novel admittance control, which works in task space. The admittance control has the form of PID, and does not need the inverse kinematic and the dynamic model of the exoskeleton. The experimental results show that both the design and the controller work well for the upper limb exoskeleton. Our further works will extend the design and controller to a 7-DoF upper limb exoskeleton.

References

[1] C. P. Joel, J. Rosen and S. Burns, Upper-limb powered exoskeleton design, *IEEE Transactions on Mechatronics*, 12 (4) (2007) 408-417.

[2] Z. Tang, K. Zhang, S. Sun and Z. Gao, An upper-limb power-assist exoskeleton using proportional myoelectric control, *Sensors*, 14 (2014) 6677-6694.

[3] H. Shing and S. Xi, Exoskeleton robots for upper-limb rehabilitation: State of the art and future prospects, *Medical Engineering & Physics*, 34 (3) (2012) 261-268.

[4] A. M. Dollar and H. Herr, Lower extremity exoskeletons and active orthoses: Challenges and state-of-the-art, *IEEE Transactions on Robotics*, 24 (1) (2008) 1-15.

[5] H. Kazerooni and R. Steger, The Berkeley lower extremity exoskeleton, *Journal of Dynamic Systems, Measurements, and Control-Transactions of the ASME*, 128 (2006) 14-25.

[6] H. Kim and J. Rosen, Predicting redundancy of a 7 DOF upper limb exoskeleton toward improved transparency between human and robot, *Journal of Intelligent & Robotic Systems*, Feburary (2015).

[7] J. J. Craig, *Introduction to robotic mechanics and control,* 3rd Edition, Prentice Hall, Upper Saddle River (2005).

[8] P. Culmer, A. Jackson, M. C. Levesley, J. Savage, R. Richardson, J. A. Cozens and B. B Bhakta, An admittance control scheme for a robotic upper-limb stroke rehabilitation system, *27th Annual Conference on Engineering in Medicine and Biology* (2005) 5081-5084.

[9] P. Maciejasz and J. Eschweiler, A survey on robotic devices for upper limb rehabilitation, *Journal of Neuro Engineering and Rehabilitation*, 11 (3) (2014).

[10] S. Moubarak, M. T. Pham, T. Pajdla and T. Redarce, Design and modeling of an upper extremity exoskeleton, *11th International Congress on Medical Physics and Biomedical Engineering*, Munich, Germany (2009) 476-482.

[11] J. T. Wen and S. Murphy, Stability analysis of position and force control for robot arms, *IEEE Trans. Automat. Contr.*, 36 (1991) 365-371.

[12] S. Ali and M. Dehghana, Adaptive hybrid force/position control of robot manipulators using an adaptive force estimator in the presence of parametric uncertainty, *Advanced Robotics*, 29 (4) (2015).

[13] M. Raibert and J. Craig, Hybrid position/force control of manipulators, *ASME J. Dynam. Syst., Meas., Contr.*, 102 (1981) 126-132.

[14] N. Hogan, Impedance control: An approach to manipulation, PartsI--III, *ASME J. Dynam. Syst., Meas., Contr.,* 107 (1985) 1-24.

[15] W. Yu, J. Rosen and X. Li, PID admittance control for an upper limb exoskeleton, *2011 American Control Conference,* San Francisco, USA (2011) 1124-1129.

[16] T. Tsuji and Y. Tanaka, Tracking control properties of human-Robotic systems based on impedance control, *IEEE Trans. Systems, Man, and Cyberbetucs-Part A*, 35 (4) (2005) 523-535.

[17] H. Kim, L. M. Miller, I. Fedulow, G. Abrams, N. Byl and J. Rosen, Kinematic data analysis for post stroke patients following bilateral versus unilateral rehabilitation with an upper limb wearable robotic system, *IEEE Transactions on Neural System and Rehabilitation Engineering*, 21 (2013) 153-164.

[18] M. Simkins, A. Al-Refai and J. Rosen, Upper limb joint space modeling of stroke induced synergies using isolated and voluntary arm perturbations, *IEEE Transactions on Neural System and Rehabilitation Engineering*, 22 (3) (2014) 491-500.

Javier Garrido is a Ph.D. student in the Automatic Control Department at Cinvestav-IPN. He received his undergraduate degree in Electronic Engineering in 2002 and M.S. in automatic control in 2004 from Cinvestav-IPN. His research interests include learning and interaction in robotic systems.

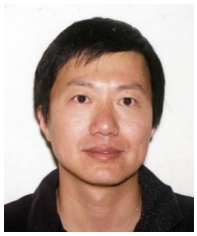

Wen Yu received the B.S. degree from Tsinghua University, Beijing, China in 1990 and the M.S. and Ph.D. degrees, both in Electrical Engineering, from Northeastern University, Shenyang, China, in 1992 and 1995, respectively. Since 1996, he has been with CINVESTAV-IPN, Mexico City, Mexico, where he is currently a Professor with the Departamento de Control Automatico. Dr. Wen Yu serves as an associate editor of Neurocomputing, and Journal of Intelligent and Fuzzy Systems. He is a member of the Mexican Academy of Sciences.

Xiaoou Li received the B.S. and the Ph.D. degree in applied mathematics and electrical engineering from Northeastern University, China, in 1991 and 1995. From 1998 to 1999, she was an associate professor of computer science at Centro de Instrumentos-UNAM. Since 2000, she has been a professor of computer science at Sección de Computación, Departamento de Ingeniería Eléctrica, CINVESTAV-IPN, México. Her research interests include Petri net theory and application, neural networks, advanced database systems, computer integrated manufacturing and discrete event systems.